LETTERS

The changing phases of extrasolar planet CoRoT-1b

Ignas A. G. Snellen[1], Ernst J. W. de Mooij[1] & Simon Albrecht[1]

Hot Jupiters are a class of extrasolar planet that orbit their parent stars at very short distances. They are expected to be tidally locked, which can lead to a large temperature difference between their daysides and nightsides. Infrared observations of eclipsing systems have yielded dayside temperatures for a number of transiting planets[1–5]. The day–night contrast of the transiting extrasolar planet HD 189733b was 'mapped' using infrared observations[6,7]. It is expected that the contrast between the daysides and nightsides of hot Jupiters is much higher at visual wavelengths, shorter than that of the peak emission, and could be further enhanced by reflected stellar light. Here we report the analysis of optical photometric data[8] obtained over 36 planetary orbits of the transiting hot Jupiter CoRoT-1b. The data are consistent with the nightside hemisphere of the planet being entirely black, with the dayside flux dominating the optical phase curve. This means that at optical wavelengths the planet's phase variation is just as we see it for the interior planets in the Solar System. The data allow for only a small fraction of reflected light, corresponding to a geometric albedo of <0.20.

The Convection, Rotation and Planetary Transit (CoRoT) satellite monitored the extrasolar planet CoRoT-1b nearly continuously for 55 days, among ~12,000 other stars in its fields of view[9]. The time sampling was 512 s during the first 30 days and 32 s for the remainder of the observations, providing a light curve with nearly 69,000 data points covering 36 planetary orbital periods ($P = 1.509$ d). A prism in front of the extrasolar-planet CCDs (charge-coupled devices) produces small spectra for each star, on which aperture photometry is performed in three bands (red, green and blue)[8]. This is done on board to comply with the available telemetry volume. The transmission curves of the three bands are different for each targeted star. They depend on the template chosen for the on-board aperture photometry, which is based on the effective temperature of the star and its position on the CCD. The Earth has a significant influence on the photometric performance of the satellite and introduces relevant perturbations on timescales of the satellite orbital period (103 min) and the 24-h day. Most of these effects were corrected for before the data release for the general astronomy community[10].

For a detailed description of the data analysis, we refer the reader to the Supplementary Information. Concentrating on the data from the red-channel passband, we rejected outlier data points and removed residual instrumental effects on the timescale of the orbital period of the satellite and the 24-h day. The final, corrected and partly resampled light curve contains 7,883 data points with a relative standard deviation of 1.0×10^{-3} and correlated noise estimated at a level of $\sim 1.2 \times 10^{-4}$, which decreases significantly when the signal is averaged over 34 transits. In strong contrast to the red-channel data, the light curves from the green and blue channels unfortunately exhibit ramps, sudden jumps and high levels of correlated noise, which make them unusable for the analysis carried out here. The short-wavelength cut-off of the red-channel passband was determined from the overall transmission curve for the telescope–CCD combination[8] multiplied with a Kurucz model spectrum[11] of the host star, which was compared with the fraction of photons collected in the red channel. This results in a wavelength cut-off of 560 nm and an effective wavelength of 710 nm.

The final, corrected light curve (Fig. 1), folded over the orbital period of the planet and binned in phase over intervals of 0.05, shows a distinct rise in flux over the first half of the orbit, followed by a dip at an orbital phase of 0.5 and a significant decrease during the second half of the orbit. This is entirely consistent with the dayside hemisphere rotating into view, being eclipsed by the star and rotating out

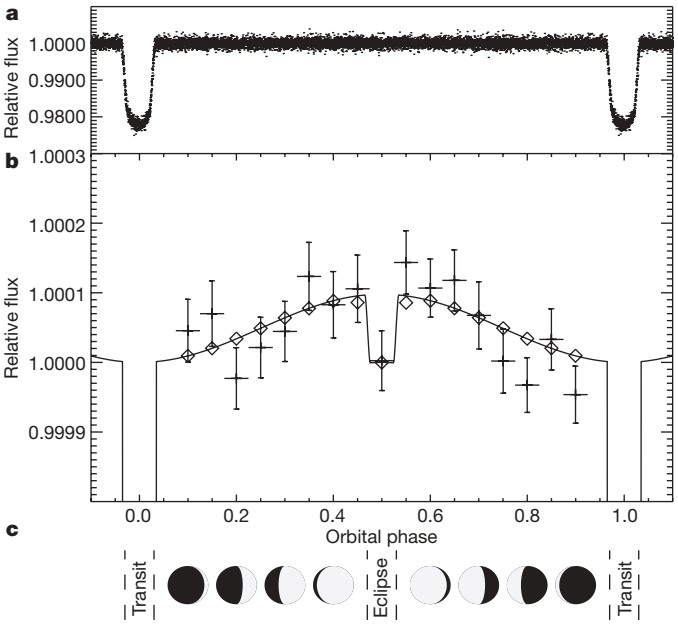

Figure 1 | Optical phase variation for CoRoT-1b centred on the planetary eclipse. Background-subtracted photometry is shown from 55 days of CoRoT monitoring in its red channel, after the rejection of $>3\sigma$ outliers and corrections for perturbations on the 103-min orbital timescale of the satellite and the 24-h day. **a**, **b**, The same data is shown in each panel, phase-folded over the planetary orbital period, $P = 1.5089557$ d. In **b**, the data are binned in phase over intervals of 0.05 (showing the 1σ error bars as determined from the scatter in the individual data points), and the scale of the y axis is magnified by a factor of ~200. The data are consistent with the dayside hemisphere rotating into view, being eclipsed by the star and rotating out of view again (**c**). The unbinned data are fitted with a model assuming uniform surface brightnesses for the dayside and nightside hemispheres; this is indicated by the solid curve. The ratio of integrated flux from the dayside hemisphere to stellar flux, as determined from the planetary eclipse depth and the phase variation, is found to be $(1.26 \pm 0.33) \times 10^{-4}$. The ratio of the flux from the nightside hemisphere to stellar flux, as determined from the difference between the secondary-eclipse depth and the amplitude of the phase variation, is found to be $<3.0 \times 10^{-5}$ at 1σ ($<5.9 \times 10^{-5}$ at 2σ) and is consistent with the hemisphere being entirely black. This means that the phase variation is just as we see it for the interior planets in the Solar System. **c**, Sketch of the phase variation.

[1]Leiden Observatory, Leiden University, Postbus 9513, 2300 RA Leiden, The Netherlands.

of view again. The amount of light received from the system at the moment the planet is eclipsed is similar to that when the nightside of the planet is in full view. This means that to within the observational uncertainties we receive no light from the nightside of the planet.

We fitted the light curve with a three-parameter model using a chi-squared analysis, assuming a homogeneous surface brightness for each of the hemispheres. The first parameter, R_{Day}, is the contrast ratio between the planet dayside flux and the stellar flux. The second parameter, $F_{N/D}$, denotes the ratio of nightside to dayside flux. A third parameter represents the flux of the star. We determine the two relevant parameters to be $R_{Day} = (1.26 \pm 0.33) \times 10^{-4}$ (with a null detection rejected at the $\sim 4\sigma$ confidence level) and $F_{N/D} = 0$ (a best-fit value), with upper limits of $F_{N/D} < 0.24$ at 1σ and $F_{N/D} < 0.47$ at 2σ, meaning that the integrated light from the nightside hemisphere is $<24\%$ (1σ) or $<47\%$ (2σ) of that from the dayside hemisphere. The influence of correlated noise was assessed by also fitting the model to a light curve with 1-h bins, for which the error of each binned point was calculated from the variation of the points at the same orbital phase over all periods. In this way, R_{Day} was determined to be slightly higher, $(1.47 \pm 0.40) \times 10^{-4}$, at a lower significance. In addition, we performed a Markov-chain Monte Carlo simulation, which yielded $R_{Day} = (1.40 \pm 0.33) \times 10^{-4}$ (Supplementary Information). Both R_{Day} and $F_{N/D}$ are influenced by the phase variation and the eclipse depth, but in different ways. Whereas the eclipse depth is a direct measure of R_{Day}, and the phase variation places a lower limit on it, it is the ratio of phase variation over the eclipse depth that governs $F_{N/D}$. The entire phase curve contributes to the estimates of R_{Day} and $F_{N/D}$, including the points near the transit.

The high level of irradiation from the nearby host star is a major factor in determining the atmospheric properties of a hot Jupiter. There is mounting evidence, both theoretical and observational, that differences in incident star flux between planets lead to at least two distinct classes of hot-Jupiter atmospheres, depending on whether or not their atmospheres contain highly absorbing substances such as gaseous titanium oxide and vanadium oxide (refs 12–19). These hot Jupiters are called 'pM-' and 'pL-class' planets[12], analogous to the M- and L-type stellar dwarfs, and the two classes are expected to have very different spectra and dayside-to-nightside circulations.

The pM-class planets, with high levels of irradiation, are thought to be warm enough to prevent condensation of titanium- and vanadium-bearing compounds. This leads to absorption of incident flux by titanium oxide and vanadium oxide at low pressure and, subsequently, a temperature inversion in the planets' stratospheres. These planets are expected to appear anomalously bright in the infrared, and to exhibit molecular bands in emission rather than in absorption[12–15]. Broadband infrared secondary-eclipse measurements for HD 209458b, a pM-class planet thought to be just above the pM–pL boundary, are indeed best explained by the presence of thermal inversion and water emission bands[14,19]. In addition, the broadband infrared spectrum of the even warmer planet TrES-4b is also best fitted with models assuming a temperature inversion in its atmosphere[17].

In the atmospheres of planets that receive less stellar flux (pL-class planets such as HD 189733b), titanium and vanadium are expected to be condensed out; the atmospheres therefore should not exhibit thermal inversion. The recent infrared spectrum of HD 189733b indeed shows strong water absorption and is best matched with models that do not include an atmospheric temperature inversion[16].

Whether or not the incident stellar flux is absorbed in a planet's stratosphere strongly influences the ratio of radiative timescales to expected dynamical timescales, and determines to what extent the absorbed energy is redistributed to the planet's nightside[12–14]. The cooler, pL-class, planets absorb incident flux deep in the atmosphere where the atmospheric dynamics are more likely to redistribute absorbed energy, leading to cooler daysides, warmer nightsides and strong jet flows resulting in significant phase shifts in their thermal emission light curves. Indeed, the pL-class planet HD 189733b is observed to have dayside–nightside temperature differences of ~ 240 K at both 8 and 24 μm, accompanied by a phase shift of 20–30° (refs 6, 7). For pM-class planets, the absorbed energy is reradiated before it can be transported to the nightside, resulting in large dayside–nightside temperature contrasts and negligible phase shifts in their thermal emission light curves. Large day–night contrasts have been found for two pM-class planets, υ Andromedae b[20] and HD 179949b[18], although a detailed interpretation is hampered because both systems are non-transiting and their orbital inclinations and planet radii are unknown.

CoRoT-1b is a strongly irradiated planet and should therefore fall well within the pM class. The measured difference between the dayside and nightside fluxes, each relative to the stellar flux, is $(1.26 \pm 0.36) \times 10^{-4}$, meaning that if there is no reflective component in the red-channel light curve, the redistribution fraction, P_n, which is the fraction of absorbed stellar radiation that is transported to the nightside of the planet[21], has an upper limit of $P_n < 0.22$ at 2σ ($P_n < 0.39$ at 3σ), in line with the low distribution fractions expected for pM-class planets. In addition, there is no evidence for a phase shift in the light curve. Therefore, if CoRoT-1b has a low albedo, it exhibits all the characteristics expected of a pM-class planet. We measure its hemisphere-averaged dayside brightness temperature to be 2390 ± 90 K. Assuming a uniform hemispheric emission, the maximum possible brightness temperature is slightly lower, at $\sim 2{,}260$ K

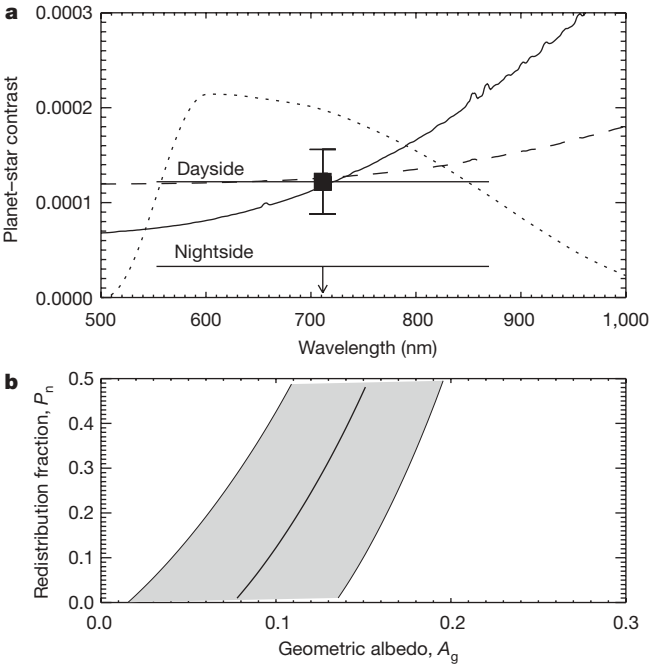

Figure 2 | The optical planet–star contrast compared with models. a, The planet–star contrast as determined from the phase variation and the planetary eclipse for the dayside and nightside of CoRoT-1b (with 1σ error bars), together with the arbitrarily scaled passband of the red-channel data (dotted line). **b**, The allowed ranges for A_g, the geometric albedo for reflected light, and for P_n, the redistribution fraction that indicates how much of absorbed stellar radiation is transported to the nightside of the planet. Here we assume wavelength-independent Lambert scattering. To obtain the planet–star contrast expected for a given combination of A_g and P_n, first the Planck curve for the planet and the Kurucz model spectrum for the primary star were separately multiplied by the transmission function of the red-channel passband and integrated over wavelength. These integrated fluxes were multiplied by their respective surface areas and the ratio was taken. This was subsequently added to a possible reflective component. The solid and dashed lines in **a** show the two most extreme cases that perfectly fit the measured planet–star contrast: $P_n = 0.0$, $A_g = 0.08$ and $P_n = 0.5$, $A_g = 0.15$. Within the 1σ uncertainty in the dayside planet–star contrast, the geometric albedo is constrained to within the range $0.02 < A_g < 0.20$. Assuming that there is no reflected light component, the 3σ limit on the redistribution fraction is $P_n < 0.39$.

for a non-reflective planet with a redistribution fraction of $P_n = 0$. If instantaneous re-emission of absorbed radiation is assumed without advection, a maximum dayside brightness temperature of ~2,430 K is obtained, within the 1σ uncertainty limits of the measured temperature. Because this indicates that any reflective component in the planet's light curve is probably small, it means that the planet has a very low geometric albedo in CoRoT's red channel.

Both theoretical modelling and observed upper limits do imply very low reflectivity for hot Jupiters. Ground-based spectroscopy that exploits the Doppler effect to separate the spectral lines of a hot Jupiter from the lines of its parent star has yielded stringent upper limits for geometric albedos (for example $A_g < 0.12$ at 3σ for HD 75289b)[22–24]. In addition, analysis of data from the MOST satellite has yielded an upper limit of $A_g < 0.17$ at 3σ for HD 209458b[25]. In comparison, the geometric albedos of Solar System gas giant planets range from 0.41 to 0.52 (ref. 26). Theoretical modelling of extrasolar-planet atmospheres shows that many parameters can cause the low albedo of hot Jupiters, in particular the strong absorption of the alkali metals sodium and potassium (and/or the aforementioned absorption of titanium oxide and vanadium oxide), and the sizes and types of condensates in the atmospheres. In the absence of clouds, the low albedo could be due to atomic or molecular absorption[27–29].

The red-channel light curve of CoRoT-1b can also be fitted with the albedo and redistribution fraction allowed to vary freely. For this, we assumed that the geometric albedo is independent of wavelength (λ) and is related to the Bond albedo by $A_g(\lambda) = 2A_B/3$, as for a diffusely scattering (Lambert) sphere. We found that in the context of this model the variation in planet–star contrast can be explained by a geometric albedo of 0.02 to 0.2 for the full range of possible redistribution fractions (Fig. 2). However, assuming that the planet's albedo is at the low end of this range, in line with both theoretical modelling and observations of other hot Jupiters, the day–night temperature contrast of CoRoT-1b is high and the redistribution fraction is low, as expected for a highly irradiated planet.

This year we celebrate the 400th anniversary of the first published astronomical observations with a telescope, by Galileo Galilei. Galilei used his telescope to observe the changing phases of Venus and reveal the true configuration of the Solar System. Now, exactly four centuries later, CoRoT observations have shown the changing phases of an extrasolar planet for the first time in optical light.

Received 28 January; accepted 6 April 2009.

1. Charbonneau, D. *et al.* Detection of thermal emission from an extrasolar planet. *Astrophys. J.* **626,** 523–529 (2005).
2. Deming, D., Seager, S., Richardson, L. J. & Harrington, J. Infrared radiation from an extrasolar planet. *Nature* **434,** 740–743 (2005).
3. Harrington, J., Luszcz, S., Seager, S., Deming, D. & Richardson, L. The hottest planet. *Nature* **447,** 691–693 (2007).
4. Sing, D. K. & Lopez-Morales, M. Ground-based secondary eclipse detection of the very-hot Jupiter OGLE-TR-56b. *Astron. Astrophys.* **493,** L31–L34 (2009).
5. de Mooij, E. J. W. & Snellen, I. A. G. Ground-based K-band detection of thermal emission from the exoplanet TrES-3b. *Astron. Astrophys.* **493,** L35–L38 (2009).
6. Knutson, H. A. *et al.* A map of the day–night contrast of the extrasolar planet HD 189733b. *Nature* **447,** 183–186 (2007).
7. Knutson, H. *et al.* Multiwavelength constraints on the day-night circulation patterns of HD 189733b. *Astrophys. J.* **690,** 822–836 (2009).
8. Auvergne, M. Bodin, P. Boisnard, L., Buey, J., Chaintreuil, S. & CoRoT team. The CoRoT satellite in flight: description and performance. *Astron. Astrophys*. (in the press); preprint at ⟨http://arxiv.org/abs/0901.2206⟩ (2009).
9. Barge, P. *et al.* Transiting exoplanets from the CoRoT space mission. I. CoRoT-Exo-1b: a low-density short-period planet around a G0V star. *Astron. Astrophys.* **482,** L17–L20 (2008).
10. Samadi, R. *et al.* Extraction of the photometric information: corrections. Preprint at ⟨http://arXiv.org/astro-ph/0703354⟩ (2007).
11. Kurucz, R. *ATLAS9 Stellar Atmosphere Programs and 2 km/s Grid.* (Kurucz CD-ROM No. 13, Smithsonian Astrophysical Observatory, 1993).
12. Fortney, J., Lodders, K., Marley, M. & Freedman, R. A unified theory for the atmospheres of the hot and very hot Jupiters: two classes of irradiated atmospheres. *Astrophys. J.* **678,** 1419–1435 (2008).
13. Cooper, C. & Showman, A. Dynamic meteorology at the photosphere of HD 209458b. *Astrophys. J.* **629,** L45–L48 (2005).
14. Showman, A. *et al.* Atmospheric circulation of hot Jupiters: coupled radiative-dynamical general circulation model simulations of HD 189733b and HD 209458b. *Astrophys. J.* (submitted); preprint at ⟨http://arXiv.org/abs/0809.2089⟩ (2008).
15. Burrows, A., Hubeny, I., Budaj, J., Knutson, H. & Charbonneau, D. Theoretical spectral models of the planet HD 209458b with a thermal inversion and water emission bands. *Astrophys. J.* **668,** L171–L174 (2007).
16. Grillmair, C. *et al.* Strong water absorption in the dayside emission spectrum of the planet HD 189733b. *Nature* **456,** 767–769 (2008).
17. Knutson, H., Charbonneau, D., Burrows, A., O'Donovan, F. & Mandushev, G. Detection of a temperature inversion in the broadband infrared emission spectrum of TrES-4. *Astrophys. J.* **691,** 866–874 (2009).
18. Cowan, N., Agol, E. & Charbonneau, D. Hot nights on extrasolar planets: mid-infrared phase variations of hot Jupiters. *Mon. Not. R. Astron. Soc.* **379,** 641–646 (2007).
19. Knutson, H., Charbonneau, D. & Allen, L. The 3.6–8.0 μm broadband emission spectrum of HD 209458b: evidence for an atmospheric temperature inversion. *Astrophys. J.* **673,** 526–531 (2008).
20. Harrington, J. *et al.* The phase-dependent infrared brightness of the extrasolar planet υ Andromedae b. *Science* **314,** 623–626 (2006).
21. Burrows, A., Budaj, J. & Hubeny, I. Theoretical spectra and light curves of close-in extrasolar giant planets and comparison with data. *Astrophys. J.* **678,** 1436–1457 (2008).
22. Collier Cameron, A., Horne, K., Penny, A. & Leigh, C. A search for starlight reflected from υ And's innermost planet. *Mon. Not. R. Astron. Soc.* **330,** 187–204 (2002).
23. Leigh, C. *et al.* A search for starlight reflected from HD 75289b. *Mon. Not. R. Astron. Soc.* **346,** L16–L20 (2003).
24. Leigh, C., Collier Cameron, A., Horne, K., Penny, A., &. James, D. A new upper limit on the reflected starlight from τ Bootis b. *Mon. Not. R. Astron. Soc.* **344,** 1271–1282 (2003).
25. Rowe, J. F. *et al.* The very low albedo of an extrasolar planet: MOST space-based photometry of HD 209458. *Astrophys. J.* **689,** 1345–1353 (2008).
26. Cox, A. N. in *Allen's Astrophysical Quantities* 4th edn (ed. Cox, A. N.) Ch. 1 (Athlone, 2000).
27. Seager, S., Whitney, B. A. & Sasselov, D. D. Photometric light curves and polarization of close-in extrasolar giant planets. *Astrophys. J.* **540,** 504–520 (2000).
28. Green, D., Matthews, J., Seager, S. & Kuschnig, R. Scattered light from close-in extrasolar planets: prospects of detection with the MOST satellite. *Astrophys. J.* **597,** 590–601 (2003).
29. Hood, B., Wood, K., Seager, S. & Collier Cameron, A. Reflected light from three dimensional exoplanetary atmospheres and simulations of HD 209458b. *Mon. Not. R. Astron. Soc.* **389,** 257–269 (2008).

Supplementary Information is linked to the online version of the paper at www.nature.com/nature.

Acknowledgements We thank the CoRoT team for making the CoRoT data, which forms the basis of this study, publicly available in a high-quality and comprehensible way. The CoRoT space mission, launched on 27 December 2006, was developed and is operated by the Centre National D'Études Spatial, with participation of the science programmes of the European Space Agency, the European Space Research and Technology Centre and the Research and Scientific Support Department, Austria, Belgium, Brazil, Germany and Spain. We thank R. Le Poole for discussions.

Author Information Reprints and permissions information is available at www.nature.com/reprints. Correspondence and requests for materials should be addressed to I.A.G.S. (snellen@strw.leidenuniv.nl).